

Efficient magnetic CoFe_2O_4 nanocrystal catalyst for aerobic oxidation of cyclohexane prepared by sol–gel auto-combustion method: effects of catalyst preparation parameters

Jinhui Tong · Xiaodong Cai · Haiyan Wang ·
Chungu Xia

Received: 23 January 2013 / Accepted: 3 April 2013 / Published online: 9 April 2013
© Springer Science+Business Media New York 2013

Abstract Six magnetic spinel-type CoFe_2O_4 samples were prepared in the form of powder by a simple sol–gel auto-combustion method from precursor solutions with different metal concentrations ($0.1\text{--}0.3\text{ mol L}^{-1}$) and pH values ($<1\text{--}10$). The samples were characterized by X-ray diffraction, Fourier transform infrared spectrophotometry, transmission electron microscopy and N_2 -physisorption. Their catalytic performances for oxidation of cyclohexane were evaluated using oxygen as oxidant in the absence of solvents. The results show that pH values and metal concentrations of precursor solutions play important roles in the sizes, dispersions and morphologies of the CoFe_2O_4 nanoparticles, and thus in their catalytic performances. The sample resulted from precursor solution under the conditions of $\text{pH} = 7$ and metal concentration = 0.1 mol L^{-1} with the largest surface area, exhibited the best catalytic performance with the highest cyclohexane conversion of 13.7 % and selectivity of 93.9 % for cyclohexanol and cyclohexanone. The CoFe_2O_4 nanocrystal is also found an efficient catalyst for oxidation of aliphatic and aromatic alkenes.

Keywords Magnetic cobalt ferrite · Metal concentration · pH value · Cyclohexane oxidation

1 Introduction

Although there have been numerous advances in oxidation of hydrocarbons using molecular oxygen, the development of more effective and selective catalysts for oxidation of inactive carbon–hydrogen bonds, in saturated hydrocarbons, remains a challenge in oxidation chemistry [1, 2]. Oxidation of cyclohexane is of great importance due to large demand for the products of cyclohexanone and cyclohexanol (K/A oil), which are important raw materials for the production of adipic acid and caprolactam. Adipic acid and caprolactam are most often used in the manufacture of nylon-6 and nylon-66 polymers [3, 4]. However, oxidation of cyclohexane has shown the least efficiency in almost all major industrial processes [5]. Oxidation of cyclohexane in the present industrial process is carried out at $\sim 150\text{ }^\circ\text{C}$ and 1–2 MPa pressure using metal cobalt salt or metal–boric acid as homogeneous catalyst. The drawback of this process is that very low conversion of cyclohexane (3–6 %) is achieved in order to maintain high selectivity (75–80 %) for the K/A oil [6]. Great efforts have been made to enhance the efficiency of this process in the past years [7–11]. However, owing to the use of large amounts of solvents and/or reducing agents as well as harsh reaction conditions, it is still difficult to apply the techniques developed at laboratory to industrial processes [7, 8, 12]. So, it becomes very necessary to develop a more effective catalyst and apply to the current industrial process. Oxidation of cyclohexane heterogeneously using molecular oxygen without any solvents or reducing agents

J. Tong · X. Cai · H. Wang
Key Laboratory of Eco-Environment-Related Polymer Materials,
Ministry of Education, Lanzhou 730070, People's Republic of
China

J. Tong · X. Cai · H. Wang
Key Laboratory of Gansu Polymer Materials, College of
Chemistry and Chemical Engineering, Northwest Normal
University, Lanzhou 730070, People's Republic of China

C. Xia (✉)
State Key Laboratory of Oxo Synthesis and Selective Oxidation,
Lanzhou Institute of Chemical Physics, Chinese Academy of
Sciences, Lanzhou 730000, People's Republic of China
e-mail: cgxia@lzb.ac.cn

is particularly desirable in both economical and environmental aspects.

Magnetic nanoparticles of complex metal oxides such as spinel ferrites become more important in recent years due to both their unique properties and broad range of applications in diverse areas such as magnetic recording and separation, ferrofluid, magnetic resonance imaging, biomedicine, catalysts, gas sensors, high quality ceramics and super paramagnetic materials [13–18]. A great advantage of using magnetic ferrite nanoparticles as catalysts in liquid-phase reactions is that the catalysts are not only thermally and chemically stable in the solution medium, but also easy to be recovered because of their magnetic property. As a matter of fact, these catalysts can be separated from the reaction medium by simply placing a magnetic field on the surface of the flask [15, 16]. As a well-known spinel ferrite an hard magnetic material, Cobalt ferrite, CoFe_2O_4 has attracted much attention because of its very high cubic magnetocrystalline anisotropy, high coercivity, and moderate saturation magnetization [13, 14, 19]. Furthermore, the properties of this material (CoFe_2O_4) are highly related to their shapes and sizes, which can be adjusted through the synthesizing processes. Significant number of methods have been developed to prepare cobalt ferrite nanomaterials with different magnetic behaviors, for instance, sonochemical reactions [20, 21], mechanochemical synthesis [22–24], hydrolysis of precursors [25, 26], flow injection synthesis [27], aqueous co-precipitation [28], hydrothermal method [14] and sol-gel auto-combustion method [29, 30]. Among these techniques, sol-gel auto-combustion synthesis has been proved to be a simple and economical way to prepare nanopowders [30, 31]. Combining the advantages of chemical sol-gel and combustion processes, sol-gel auto-combustion synthesis gives rise to a thermally induced anionic redox reaction. The energy released from the reaction between oxidant and reductant is adequate to form a desirable phase within very short time [32]. The process exhibits the advantages of inexpensive precursors, a simple preparation process, and can produce highly reactive nano-sized powder [32, 33].

In our previous work [34], CoFe_2O_4 nanocrystal synthesized by sol-gel auto-combustion method was proved to be highly active and easily recovered catalyst for the oxidation of cyclohexane by molecular oxygen without addition of solvents or reductants. Since the efficiencies of this kind of catalysts closely depends on their shapes, sizes, and structures, which can be adjusted by controlling the conditions of sol-gel auto-combustion processes, the present work focuses on exploring the effects of pH values and metal concentrations of precursor solutions on the properties and catalytic performances of the CoFe_2O_4 nanoparticles.

2 Experimental

2.1 Preparation of CoFe_2O_4 nanoparticles

Nanoparticles of CoFe_2O_4 spinels were prepared based on a modified procedure described in the literature [22]. Keeping 1:1 molar ratio of metal cations to citric acid, $\text{Fe}(\text{NO}_3)_3 \cdot 9\text{H}_2\text{O}$, $\text{Co}(\text{NO}_3)_2 \cdot 6\text{H}_2\text{O}$ and citric acid were completely dissolved in distilled water under magnetically stirring to form a transparent solution. The solution was allowed to evaporate in an oil bath under continuous stir at 80–90 °C until a brown gel appeared. The gel was dried at 110 °C till a spumous xerogel was obtained. Produced xerogel was ignited at 650 °C, a self-propagating combustion process occurred and dark grey loose product was obtained after the combustion was completed. The product was pulverized in an agate mortar to obtain CoFe_2O_4 nanoparticles. pH value of the original solution is <1, and concentrated ammonia (25–28 %) was added slowly under constant stir to adjust the pH value. Six samples (**A**, **B**, **C**, **D**, **E** and **F**) from different precursor solutions were prepared as listed in Table 1 to investigate the effects of pH values and metal concentrations on the as-prepared CoFe_2O_4 nanoparticles.

The xerogels produced from different precursor solutions showed different combustion behaviors. The xerogels, except **D**, showed a fast flaming auto-combustion reaction producing large amounts of gases: the combustion started in the hottest zones of the crucible and propagated from the bottom to the top like the eruption of a volcano. The reaction was completed in 10–30 s giving rise to a dark grey voluminous product with a structure similar to a branched tree. In the case of xerogel **D**, the thermal treatment brought about a slow reaction that leads, in about 5 min, to a product of a grey dark powder. In this case the volume did not change during the reaction. The similar phenomena have also been described in the literature [31].

2.2 Catalysts characterization

X-Ray powder diffraction (XRD) of the samples was performed on a PANalytical X'Pert Pro diffractometer using $\text{Cu K}\alpha$ radiation with a scanning angle (2θ) of 10–80° and a voltage and current of 40 kV and 30 mA.

Fourier transform infrared (FT-IR) spectra of samples in KBr wafer were collected using a Nicolet Nexus 870 FT-IR spectrometer. Spectra were recorded in the 4,000–400 cm^{-1} range with a resolution of 4 cm^{-1} .

Transmission electron microscopy (TEM) micrographs of the samples were obtained using a Hitachi H-600 microscope.

Table 1 Preparation parameters, BET surface area, XRD and BET average particle sizes of the samples

Sample	Preparation parameters		BET surface area (m ² g ⁻¹)	XRD average particle size (nm)	BET average particle size (nm)
	pH value	Metal concentration (mol L ⁻¹)			
A	7	0.1	38.6	24	29
B	7	0.2	37.9	26	30
C	7	0.3	31.2	28	36
D	<1	0.1	6.2	16	185
E	3	0.1	19.0	21	60
F	10	0.1	35.8	30	32

The BET surface area measurements were performed on a Micromeritics ASAP 2010 instrument at liquid nitrogen temperature.

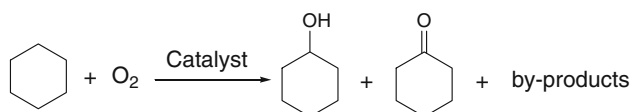
2.3 Oxidation tests

Oxidation of cyclohexane was performed in a 30 mL stainless steel autoclave equipped with a magnetic stirrer and an automatic temperature controller. In a typical reaction, 5.0 mg catalyst and 7.0 mL (65.3 mmol) cyclohexane were added to the autoclave. The autoclave was flushed three times with O₂ and pressurized to the desired pressure, then placed in the oil bath under desired temperature and stirring. After the reaction, the autoclave was cooled to room temperature and slowly depressurized. The products were identified by GC–MS and quantified by GC using toluene as the internal standard. The main by-products of the reaction are hexanedioic acid, hexanoic acid, dicyclohexyl adipate and cyclohexyl caproate (Scheme 1). Due to magnetic properties of the prepared nanoparticles, they can be attracted to the stirrer. This may somewhat lower dispersity and consequently catalytic performance of the catalyst.

3 Results and discussion

3.1 XRD analysis

Figure 1 shows the XRD patterns of the as-synthesized samples. For samples A–D, the position and relative intensity of all diffraction peaks match well with standard

**Scheme 1** Oxidation of cyclohexane

cobalt ferrite spinel XRD data (JCPDS NO. 22-1086). For samples E and F, however, low intensity reflections that can be ascribed to Co₂O₃ phase were observed besides of the spinel reflections.

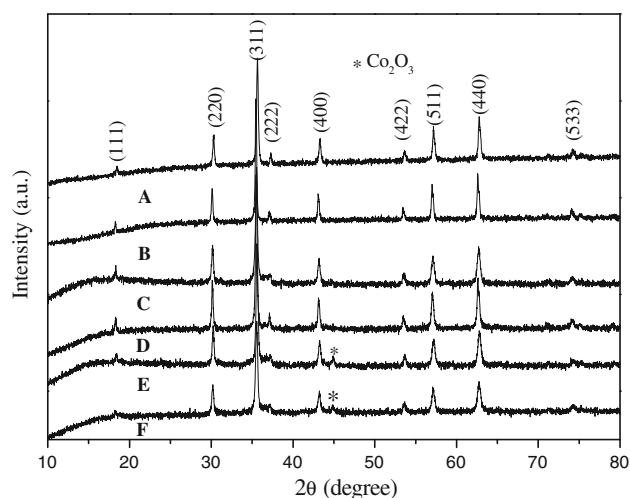
The mean particle sizes of the samples calculated by applying the Sherrer equation to [311] reflections are 24, 26, 28, 16, 21 and 30 nm for the samples A–F, respectively (Table 1). It is clear that precursor solutions with high pH values and metal concentrations are in favor of resulting in big nanoparticles. Furthermore, it shows that the particle size is more sensitive to pH value than to metal concentration.

3.2 FT-IR analysis

Fourier transform infrared spectra of the samples were displayed in Fig. 2. For each sample, a strong band associated with the Fe–O stretching vibration at around 580 cm⁻¹ is presented. It confirms the presence of the cobalt ferrite phase [31]. No characteristic bands corresponding to citric acid or NO₃⁻ appeared, and this indicates that no citric acid or NO₃⁻ is residual in the sample.

3.3 TEM analysis

Transmission electron microscopy micrographs and size distribution histograms of the samples are shown in Figs. 3 and 4, respectively. The sample A shows irregular particles with diameters about 15–40 nm, and most particles with diameters about 25 nm. The sample B shows chain-like aggregations of spherical particles and most of them with uniform size about 25 nm. The morphology of sample C exhibits a majority of irregular particles with diameters about 30 nm and a minority of the spherical analogues with diameters about 15 nm. Consideration the differences among the samples A–C in metal concentrations of

**Fig. 1** X-Ray powder diffraction patterns of the samples

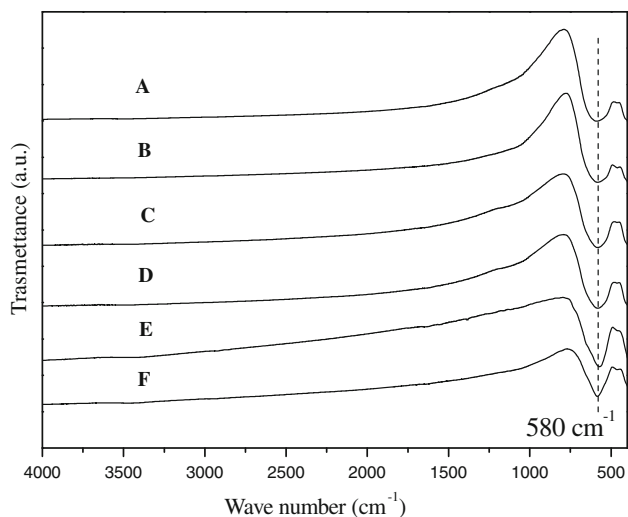


Fig. 2 Fourier transform infrared spectra of the samples

precursor solutions, it can be concluded that the sizes of the nanoparticles increase with increasing of metal concentrations (Fig. 4).

The pH values of the precursor solutions seem to have more significant effects on the sizes and morphologies of the resulted nanoparticles. As can be seen from Figs. 3 and

4, the sample D, produced from the precursor solution with the lowest pH value, shows the most serious aggregations about 50–200 nm formed mostly by small particles about 15 nm. The sample E, resulted from the precursor solution with pH 3, consists of smaller aggregations about 50–80 nm formed mostly by particles about 20–27 nm. When the pH value was improved to 10, the resulted sample F is mostly composed of nanoparticles with diameters of ~ 30 nm. Based on above facts, it can be concluded that the precursor solutions with higher pH values can produce much bigger but more uniform nanoparticles.

3.4 N₂-physisorption analysis

N₂-physisorption measurements were performed for the as-prepared samples. The BET surface areas of the samples were summarized in Table 1 together with the average particle sizes calculated by the formula $d = 6/\rho A$, where ρ is the theoretical density of the material (5.20 g cm^{-3} for CoFe₂O₄ bulk) and A is the specific surface area [31]. As for samples D and E resulted from precursor solutions with low pH values, the average particle sizes determined by BET method are much larger than those based on XRD measurements, indicating that much agglomerations exists

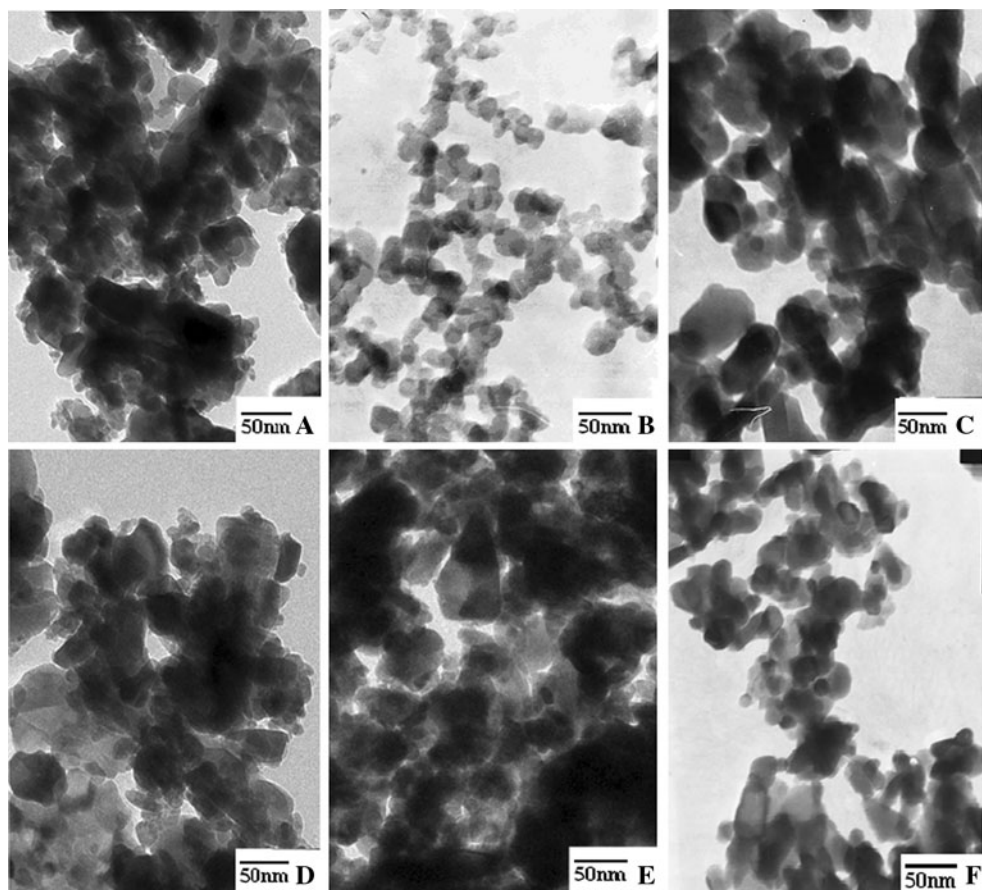


Fig. 3 Transmission electron microscopy morphologies of the samples

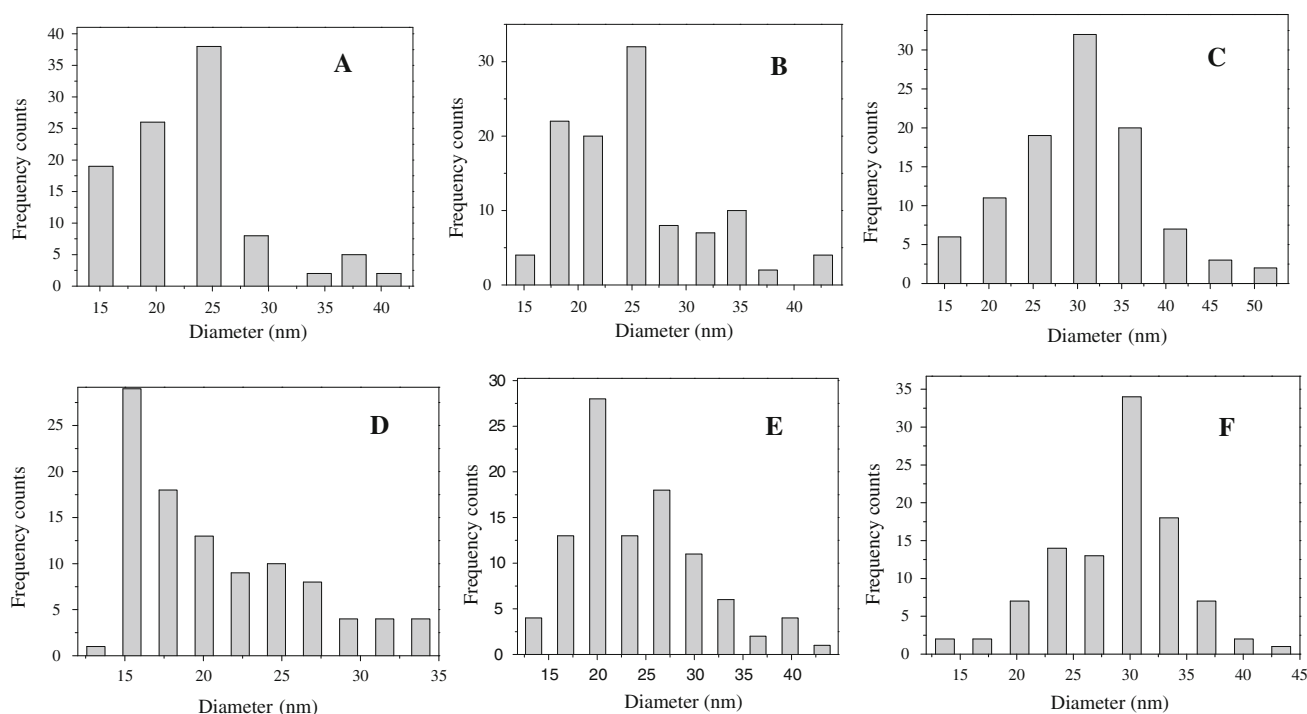


Fig. 4 Size distribution histograms of the samples

in the samples. As a result, the sample **D** has the smallest particles and, however, the lowest BET surface area because of the most extent of agglomeration. For the other samples, which were prepared from the solutions with high pH values, the average particle sizes calculated based on BET and XRD measurements are similar, indicating low degree of agglomerations in the samples. The facts are consistent with the statistical analysis of the TEM images.

According to the literature [32], when $\text{NH}_3 \cdot \text{H}_2\text{O}$ is added to the precursor solution, the excess NH_4^+ groups exists in the gel as NH_4NO_3 when the pH value is above 4. In the cases of high pH values, most of NH_4NO_3 remains in dried gels. During the drying and combustion process, the remaining NH_4NO_3 may decompose to liberate NO_x and O_2 . The produced oxygen can accelerate the combustion process and a great amount of heat releases in this reaction. This may be

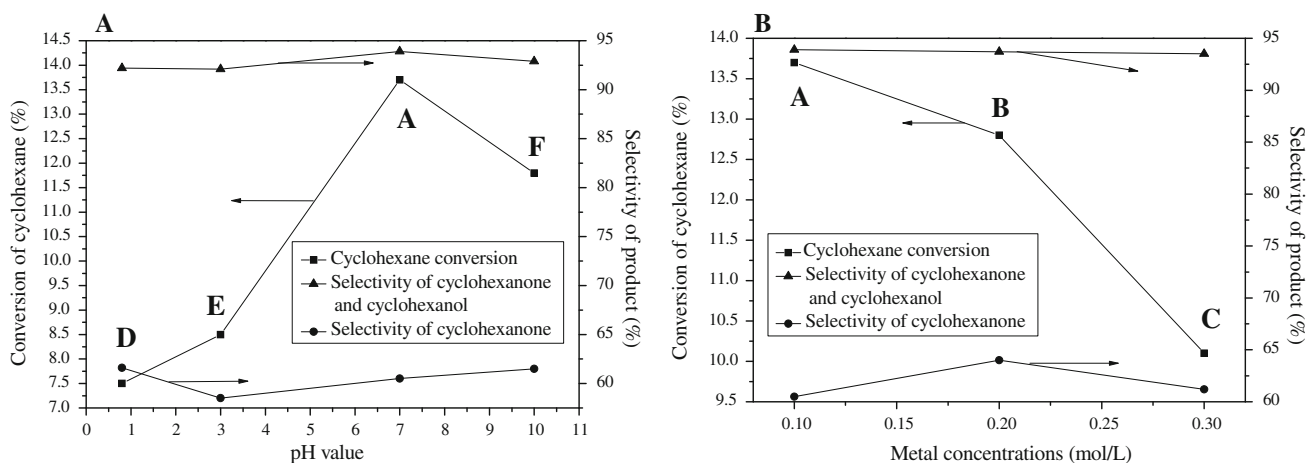

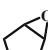
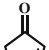
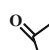

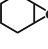
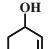
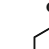
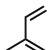

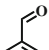

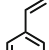

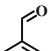


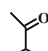
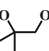
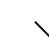
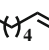
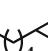

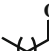

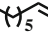
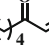
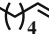
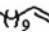
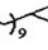
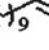
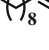


Fig. 5 Oxidation of cyclohexane catalyzed by **A** the samples **A**, **D**, **E** and **F** prepared from precursor solutions with different pH values; **B** the samples **A**, **B** and **C** prepared from precursor solutions with

different metal concentrations. Reaction conditions: cyclohexane 7.0 mL (65.3 mmol); catalyst 5.0 mg; initial oxygen pressure = 1.6 MPa; temperature = 145 °C; reaction time = 6.0 h

Table 2 Oxidation of alkenes on the sample A

Entry	Substrate	Conversion (%) ^a	Selectivity (%) ^a			
1		62.9	 (76.7)	 (11.6)	 (4.6)	Others (7.1)
2 ^b		19.3	 (2.7)	 (31.5)	 (54.3)	Others (11.5)
3 ^c		8.7	 (70.5)	 (23.3)	 (—)	Others (6.2)
4 ^d		24.6	 (—)	 (79.0)	 (8.3)	Others (12.7)
5 ^e		32.9	 (66.8)	 (16.8)	 (6.1)	Others (10.3)
6 ^e		9.2	 (22.7)	 (42.8)	 (23.8)	Others (10.7)
7 ^e		8.0	 (32.0)	 (24.2)	 (23.9)	Others (19.9)
8 ^e		4.1	 (19.2)	 (39.3)	 (35.6)	Others (5.9)

Typical reaction conditions: catalyst 10 mg (0.042 mmol); substrate 2.0 mL; acetone 10 mL; substrate/H₂O₂ = 1:1 (n/n); temperature = 60 °C; reaction time = 6.0 h

^a Entry 2–5 were quantified by GC using toluene as the internal standard, the others were quantified by GC based on the area normalization

^b 70 °C, 8 h

^c O₂ 0.1 MPa, DMF 10 mL, 90 °C, 10 h

^d 70 °C, 10 h

^e Substrate 1.0 mL

responsible for the increase in the crystallite sizes with increasing pH values. On the other hand, as a lot of gasses will be liberated from the precursors during drying and combustion, it enhances the particle dispersions and enlarges the specific surface areas.

3.5 Catalysis of the prepared catalysts for oxidation of cyclohexane

The performances of the prepared samples on oxidation of cyclohexane were evaluated under optimum conditions in our previous work [34] and the results were presented in Fig. 5. As expected, pH values and metal concentrations of precursor solutions have evident effects on catalytic performances of the resulted samples. As a result, increase of pH or decrease of metal concentration of precursor solution seems to enhance the catalytic performance of the sample when conversion of cyclohexane is concerned (Fig. 5). However, when pH is too high, as for the sample F (pH = 10), the conversion of cyclohexane dropped slightly. The same correlation is observed between BET surface areas of the samples and precursor solution parameters (Table 1). That is, cyclohexane conversions increased with the increase in the BET surface areas of the samples, possibly due to the enhancement of the contact of cyclohexane with the catalyst surface. Among the catalysts tested, the sample A, with the largest surface area, exhibited the best catalytic performance with the highest cyclohexane conversion of 13.7 % and selectivity of 93.9 % for cyclohexanol and cyclohexanone. Since Co_2O_3 is less active than CoFe_2O_4 for aerobic oxidation of cyclohexane under our experiments conditions according to our previous investigations, as for the samples E and F, the presence of minor Co_2O_3 may somewhat reduce their catalytic performances [34].

3.6 Catalysis of the prepared catalysts for oxidation of alkenes

In order to expand the applicable substrate scope of the CoFe_2O_4 nanocrystal, the sample A was chosen as a representative to investigate the activation in the oxidation of alkenes and the results were collected in Table 2. The CoFe_2O_4 sample proved to be also efficient in oxidation of both aliphatic and aromatic olefins. Especially in the oxidation of cyclopentene with H_2O_2 , high conversion of 62.9 % for cyclopentene and selectivity of 76.7 % for epoxide were achieved at 60 °C for a 6-h reaction (Table 2, Entry 1). The optimization of the reaction conditions are under investigation.

4 Conclusion

In conclusion, pH values and metal concentrations of the precursor solutions play important roles in controlling the

particle sizes, dispersions, and morphologies of the final products of CoFe_2O_4 . The special surface areas and catalytic performances are therefore affected by the parameters of the precursor solutions. The sample obtained from the precursor solution with 0.1 mol L^{-1} metal concentration at pH 7 manifests moderate particle size and the highest BET surface area, and thus the highest catalytic activities. The CoFe_2O_4 sample was also efficient for oxidation of both aliphatic and aromatic olefins. High conversions and selectivities were achieved in the oxidation of cyclopentene and α -methyl styrene. Both our previous and present work [34] has shown that this kind of catalysts exhibit excellent reusability and can be easily recovered.

Acknowledgments This work was supported by the National Science Fund for Distinguished Young Scholars of China (20625308), Scientific Research Fund of Northwest Normal University (NWNULKQN-10-28) and Program for Changjiang Scholars and Innovative Research Team in University (IRT1177).

References

1. Labinger JA (2004) *J Mol Catal A* 220:27–35
2. Crabtree RH (1995) *Chem Rev* 95:987–1007
3. Schuchardt U, Carvalho WA, Spinace EV (1993) *Synlett* 10:713–718
4. Schuchardt U, Cardoso D, Sercheli R, Pereira R, Cruz RS, Guerreiro MC, Mandelli D, Spinace EV, Fires EL (2001) *Appl Catal A* 211:1–17
5. Kesavan V, Sivanand PS, Chandrasekaran S, Koltypin Y, Gedanken A (1999) *Angew Chem Int Ed* 38:3521–3523
6. Sawatari N, Yokota T, Sakaguchi S, Ishii Y (2001) *J Org Chem* 66:7889–7891
7. Narayan RV, Kanniah V, Dhathathreyan A (2006) *J Chem Sci* 118:179–184
8. Wang HL, Li R, Zheng YF, Chen HN, Wang FS, Ma JT (2008) *Catal Lett* 122:330–337
9. Perkas N, Wang YQ, Koltypin Y, Gedanken A, Chandrasekaran S (2001) *Chem Commun* 11:988–989
10. Yuan HX, Xia QH, Zhan HJ, Lu XH, Su KX (2006) *Appl Catal A* 304:178–184
11. Tong JH, Li Z, Xia CG (2005) *J Mol Catal A* 231:197–203
12. Yu KMK, Abutaki A, Zhou Y, Yue B, He HY, Tsang SC (2007) *Catal Lett* 113:115–119
13. Xiao SH, Jiang WF, Li LY, Li XJ (2007) *Mater Chem Phys* 106:82–87
14. Zhao LJ, Zhang HJ, Xing Y, Song SY, Yu SY, Shi WD, Guo XM, Yang JH, Lei YQ, Cao F (2008) *J Solid State Chem* 181:245–252
15. Faungnawakij K, Kikuchi R, Shimoda N, Fukunaga T, Eguchi K (2008) *Angew Chem Int Ed* 47:9314–9317
16. Menini L, Pereira MC, Parreira LA, Fabris JD, Gusevskaya EV (2008) *J Catal* 254:355–364
17. Wang X, Lin Y, Zhang ZC, Bian JY (2011) *J Sol-Gel Sci Technol* 60:1–5
18. Li L (2011) *J Sol-Gel Sci Technol* 58:677–681
19. Wang Z, Fei W, Qian H, Jin M, Shen H, Jin M, Xu J, Zhang W, Bai Q (2012) *J Sol-Gel Sci Technol* 61:289–295
20. Shafi K, Gedanken A, Prozorov R, Balogh J (1998) *Chem Mater* 10:3445–3450
21. Srivastava DN, Perkas N, Gedanken A, Felner I (2002) *J Phys Chem B* 106:1878–1883

22. Ennas G, Marongiu G, Marras S, Piccaluga G (2004) *J Nanopart Res* 6:99–105
23. Manova E, Tsoncheva T, Paneva D, Mitov I, Tenchev K, Petrov L (2004) *Appl Catal A* 277:119–127
24. Shi Y, Ding J, Yin H (2000) *J Alloys Compd* 308:290–295
25. Ammar S, Helfen A, Jouini N, Fievet F, Rosenman I, Villain F, Molinie P, Danot M (2001) *J Mater Chem* 11:186–192
26. Ben Tahar L, Smiri LS, Artus M, Joudrier AL, Herbst F, Vaulay M, Ammar S, Fievet F (2007) *Mater Res Bull* 42:1888–1896
27. Hyeon T (2003) *Chem Commun* 0:927–934
28. Paik VV, Niphadkar PS, Bokade VV, Joshiw PN (2007) *J Am Chem Soc* 90:3009–3012
29. Barati MR (2009) *J Sol-Gel Sci Technol* 52:171–178
30. Zhang RJ, Huang JJ, Zhao HT, Sun ZQ, Wang Y (2007) *Energy Fuels* 21:2682–2687
31. Cannas C, Falqui A, Musinu A, Peddis D, Piccaluga G (2006) *J Nanopart Res* 8:255–267
32. Yue Z, Guo W, Zhou J, Gui Z, Li L (2004) *J Magn Magn Mater* 270:216–223
33. Ma N, Yue YH, Hua WM, Gao Z (2003) *Appl Catal A* 251:39–47
34. Tong JH, Bo LL, Li Z, Lei ZQ, Xia CG (2009) *J Mol Catal A* 307:58–63